A Summertime Severe Weather Event Occurring in the Taipei Basin

George Tai-Jen Chen[1,*], and Hung-Chi Chou[2]

ABSTRACT

A case of summertime strong convection occurring on 29 August 1999, producing hail and strong gusts in the Taipei Basin, was studied using conventional and Doppler radar data. Results showed that an upper-level cold vortex to the east of Taiwan provided strong vertical wind shear and increased potential instability favorable for the development of strong convection. Drying of the mid-troposphere was primarily responsible for the strong gusts as mid-level dry air entered the system and caused strong evaporative cooling.

It was found that the convection was triggered by sea breezes, upslope wind, and an accompanying convergent line under a weak synoptic-scale flow. It was suggested that the interaction of the sea breeze/upslope wind with the outflow from the convective system over mountain slopes was responsible for the maintenance and northwestward propagation of the system. Also, an upward dynamic pressure gradient associated with the increase in vertical shear under the influence of an upper-level cold vortex appeared to be a supportive factor for the westward propagation and intensification of this convective system. Finally, a mesovortex formed in the convective system by the tilting process in the area of strong updraft under increased environmental vertical wind shear.

(Key words: Doppler radar, Hail, Gust, Vortex, Sea breeze, Upslope wind, Outflow, Convection, Vertical shear)

1. INTRODUCTION

Thunderstorms and/or showers associated with afternoon convection are common weather

[1] Department of Atmospheric Sciences, National Taiwan University, Taipei, Taiwan, ROC

[2] CKS Aeronautical Meteorological Station, Civil Aeronautics Administration, Taipei, Taiwan, ROC

* *Corresponding author address:* Prof. George Tai-Jen Chen, Department of Atmospheric Sciences, National Taiwan University, Taipei, Taiwan, ROC; E-mail: george@george2.as.ntu.edu.tw

phenomena in summer over the Taiwan area particularly in the Taipei Basin. There was a total of 402 thunderstorm days reported in 30 years (1961 - 1990) in July and August with a mean daily probability of more than 20% chance of thunderstorm occurrence climatologically. Although afternoon thunderstorms over the Taiwan area may cause heavy rain which often produces flooding locally, it rarely causes severe weather such as hail, tornados, and strong surface gust wind. Taking strong gust wind as an example, there were only 6 cases of gust events greater than 15 $m s^{-1}$ associated with summertime afternoon thunderstorms occurring at the Sung-Shan Airport during the 12-year period (July - August 1988 - 1999) up until the present case. The strongest case among these occurred on 28 August 1988 with a gust wind of 27.5 $m s^{-1}$, followed by the present case study of 26.5 $m s^{-1}$ at 1537 LST on 29 August 1999. This case was selected not only because of the occurrence of strong gust wind, but also the occurrence of hail in adjacent areas prior to the occurrence of the gust.

Located over the subtropical area in the western North Pacific, Taiwan is affected by the East Asian summer southwesterly monsoonal flows, which are warm, moist, and potentially unstable. The frequent occurrence of summertime afternoon thunderstorms and rarely accompanying severe weather conditions are presumably due to relatively weak vertical wind shear and the very moist environment in summer. These conditions are not favorable for the formation of severe convection, tilted updraft/downdraft, and strong downdraft/cold pools (e.g., Newton and Newton 1959; Zipser 1977; Rotunno et al. 1988; Weisman 1992). Chen et al. (1990) studied severe convective storms developing over the Taiwan area in summer and suggested that westward propagating upper-level cold vortices might play an important role in changing environmental conditions and providing the forcing necessary for triggering the convection. They observed that the upper-level cold vortex not only increased both potential instability by lowering upper-level temperature and vertical wind shear by increasing upper-level wind speed, but also provide lift for convection initiation by the accompanying upper-level jet streak.

In the present case, a westward propagating upper level cold vortex moved to the southeast of Taiwan during a period of afternoon convection. The purpose of this paper is to study environmental conditions and triggering mechanism for the strong convection in this case. Also, the formation, behavior, and structure of the convective system, which produced hail and strong gusts, are investigated.

2. DATA AND ANALYSES

Radar reflectivity of vertical maximum indicator (VMI), range height indicator (RHI), and constant altitude plan position indicator (CAPPI) and radial winds observed at the Chiang Kai-Shek (CKS) International Airport Doppler radar at 0.5-h intervals on 29 August 1999 were used to study the structure and evolution of a convective system. Mesoscale analyses were carried out using surface observations obtained from the Central Weather Bureau (CWB) of Taiwan to reveal local circulations and distribution of convective rainfall. Hourly observations at the Sung-Shan Airport were used to analyze weather changes during the passage of a gust front. Rawinsonde data at Pan-Chiao (Taipei) station were used to analyze the environ-

mental conditions. These data were also used to compute the convective available potential energy (CAPE) and convective Richardson number (Ric) as defined by Weisman and Klemp (1982). Also, the surface and 300 hPa weather charts of the Japan Meteorological Agency were used to illustrate the synoptic situations. Figure 1 presents the topography over northern Taiwan and the geographical locations for the CKS International Airport, the Sung-Shan Airport, and Pan-Chiao rawinsonde station. Taipei Basin is located to the north of the Snow Mountain Range (SMR), which is oriented in an NE-SW direction over northern Taiwan.
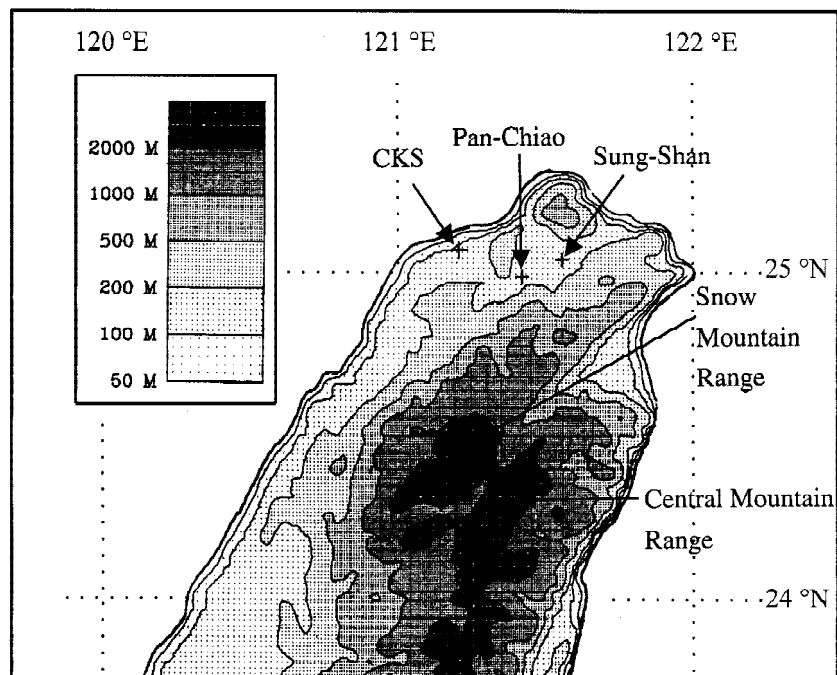

Fig. 1. Smoothed topography over northern Taiwan and locations of CKS and Sung-Shan Airports and Pan-Chiao rawinsonde station.

3. SYNOPTIC SITUATIONS

Surface analysis at 0000 UTC 29 August is presented in Fig. 2a. A weak stationary front was located roughly over the East China Sea and the Yangtze River Valley. Taiwan was not affected by this frontal system. The Pacific subtropical high pressure center was located near 37°N, 160°W with a ridge line extending southwestward passing through Taiwan into the southern China coast. A separated secondary high center was located to the east of Taiwan such that a weak pressure gradient and south-southwesterlies prevailed over Taiwan and its vicinities. Figure 2b presents the 300 hPa analysis at 0000 UTC 29 August. A weak short wave trough was located to the west of the Korean peninsula and another one over northern China.
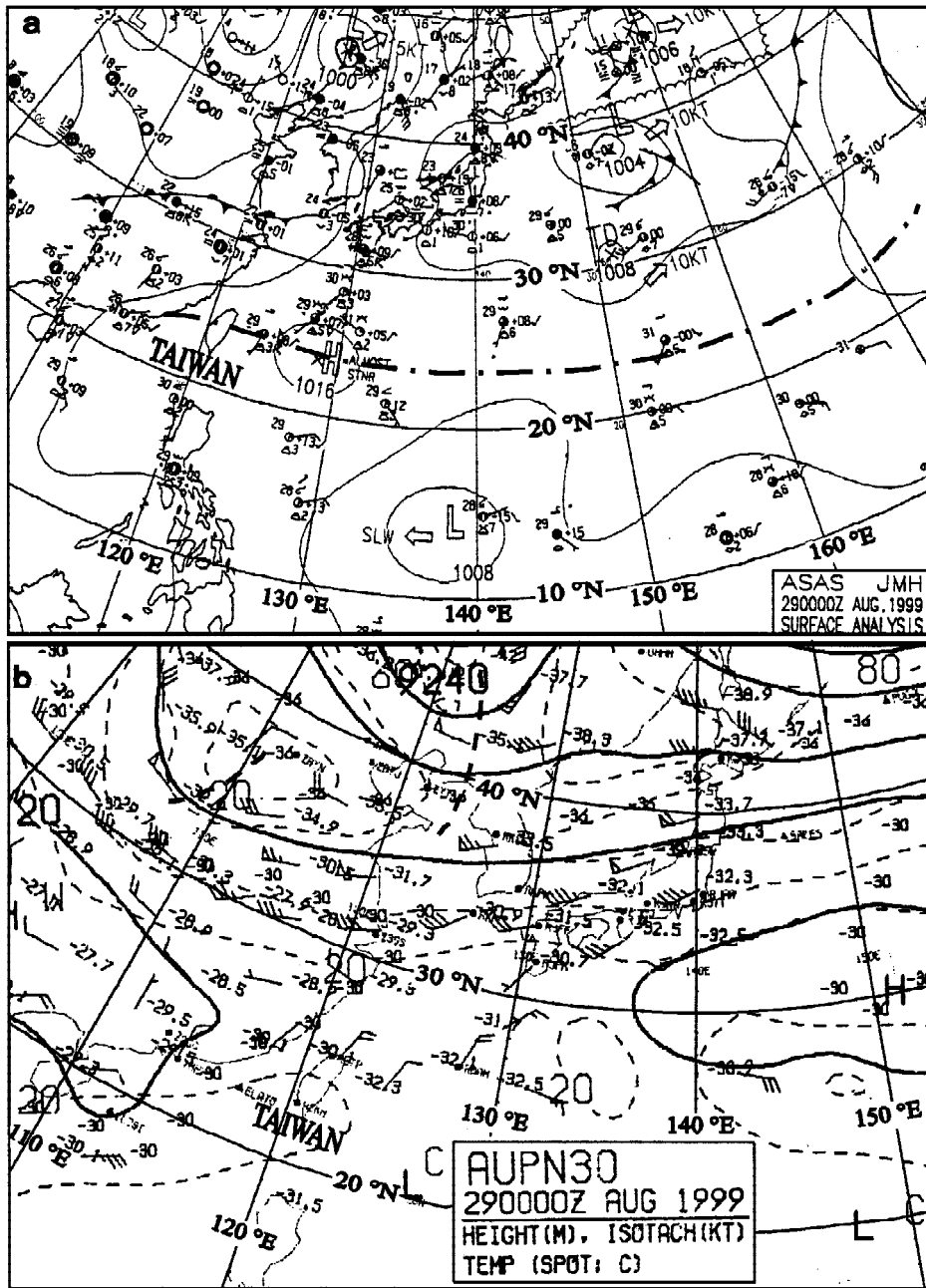
Fig. 2. (a) surface and (b) 300 hPa analyses at 0000 UTC 29 August 1999. Surface isobars analyzed at 4 hPa intervals, 300 hPa contours at 120 gpm intervals, and isotachs at 10 m s^{-1} intervals. Dash-dotted line at surface is ridge line and heavy dashed lines at 300 hPa are trough lines.

Apparently, Taiwan was not affected by the mid-latitude systems. A westward propagating cold vortex was located to the east of Taiwan such that northeasterlies prevailed over Taiwan and adjacent areas. It tended to move northward in the following time periods along the western periphery of the Pacific subtropical high.

The vertical time cross section of winds and temperatures observed at the Pan-Chiao rawinsonde station in 1200 UTC 27 - 0000 UTC 30 August is illustrated in Fig. 3. Different flow regimes occurred at upper and low levels. The flows were dominated by the easterlies/ northeasterlies/northerlies at upper levels and by southwesterlies at low levels. The increase of northeast winds at 200 - 300 hPa reflected the cold core low influence. Winds at 200 hPa increased from 7.5 m s^{-1} at 1200 UTC 27 August to a maximum of 17.5 m s^{-1} at 0000 and 1200 UTC 29 August. The vertical shear in the troposphere also reached a maximum at 0000 UTC 29 August, although it was relatively weak as compared to the wintertime environment over this area. The cold vortex influence is also manifested by a noticeable temperature decrease in the upper troposphere from 0000 to 1200 UTC 29 August.

Figure 4 presents the sounding at Pan-Chiao station at 0000 UTC 28 and 29 August. It is clear that the troposphere was drying from 28 to 29 August as indicated by the increase of dew point depression above 850 hPa. At 0000 UTC 29 August, the CAPE (1312 m^2 s^{-2}) was slightly smaller than that at 0000 UTC 28 August (1515 m^2 s^{-2}). At the same time, the convective Richardson number (Ric) was large (45) due to relatively weak vertical shear. It was much
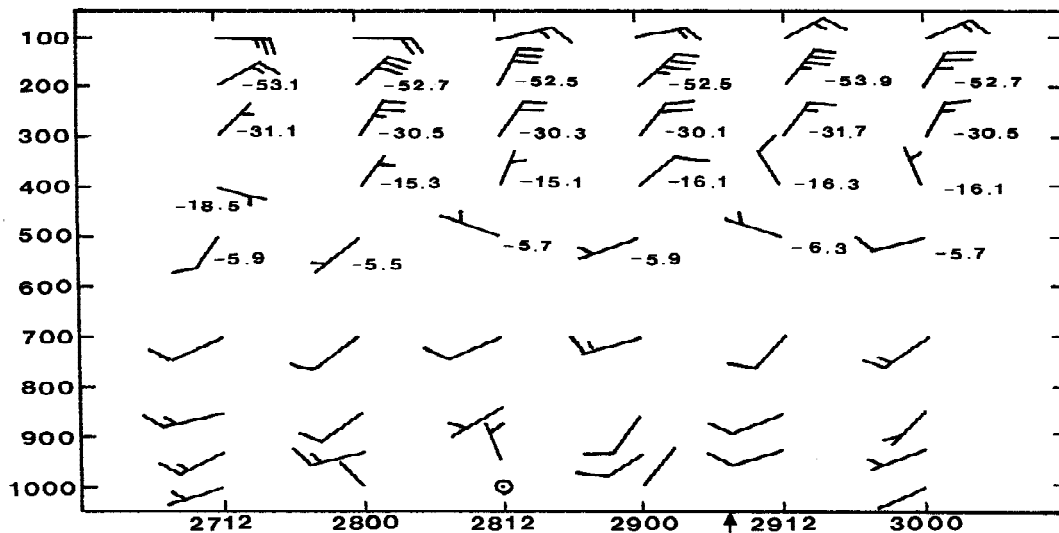

Fig. 3. Vertical time cross section of winds and temperatures (°C) at Pan-Chiao station in 1200 UTC 27 - 0000 UTC 30 August 1999. The full barb and half barb represent 5 and 2.5 m s^{-1}, respectively. Abscissa is time in UTC and ordinate is pressure in hPa. Arrow indicates the occurrence time of strong gust wind and hail.

larger than the value (Ric = 15 - 35) favorable for the occurrence of supercell thunderstorms (Weisman and Klemp 1982). Again, different flow regimes were evident at upper and low levels. The 0°C level occurred at 4.5 km slightly lower than the climatological average of about 5 km. A low melting level is favorable for hailstones to reach the ground.

4. SURFACE MESOANALYSES

Streamline and isohyet analyses are presented in Fig. 5 for the period of 0000 - 0800 UTC 29 August. Local time (LST) is UTC plus 8 hours. Offshore flows associated with land breezes/ downslope winds were observed along the northern and northwestern coastal area at 0000 UTC. An anticyclonic center existed over the Snow Mountain Range (SMR) and cyclonic circulations developed along the eastern and western coastal areas. At 0300 UTC, sea breezes prevailed as evidenced by onshore flows along coastal areas and upslope winds that developed over the western and eastern slopes of the SMR and Central Mountain Ranges (CMR). Meanwhile, cyclonic vortices formed over areas along the northern coast and on the western slope of the SMR.

At 0600 UTC, a convergent line formed along the SMR and another one formed over its western slope where a convective rainfall center of 6 mm h^{-1} was observed. At 0700 UTC, a primary convective rainfall center with a maximum value of 32.5 mm h^{-1} occurred over the SMR. Although sea breezes still prevailed along the western coastal areas, an anticyclonic outflow center formed over the area of this maximum rainfall center. Over the western slope of the SMR, the rainfall center appeared to move northeastward from its previous location with intensity increasing to 20 mm h^{-1}. At 0800 UTC, the primary rainfall center moved north-westward to the northern slope of the SMR with a maximum value increased to 48.5 mm h^{-1}. The anticyclonic outflow circulation continued to develop over the rainfall area such that off-shore flows dominated over the northern and northeastern coastal areas. The secondary rain-fall center over the western slope decreased in intensity to a value of 5.5 mm h^{-1} over the area where the sea breezes/upslope winds still prevailed.

Figure 6 presents the surface hourly observations at the Sung-Shan Airport on 29 August. A weak sea breeze from the northwest appeared at 1000 LST and prevailed until 1500 LST when it started to veer to north-northeast. During this period, a fall in pressure was accompa-nied by a slight increase in temperature while dew point temperature remained relatively steady. After 1500 LST, the Sung-Shan Airport experienced an outflow from the primary convective rainfall center as presented in Figs. 5d and e. Wind further veered from north-northeast to the southeast as temperature and dew point dropped rapidly. A remarkable temperature drop took place at 1500 - 1548 LST with a value of 10.5°C $(48 \text{ min})^{-1}$, indicating strong evaporative cooling in the convective downdraft. Hail was observed over the eastern section of Taipei City at 1515 LST and a southeast wind of 16.5 m s^{-1} was observed with a strong gust of 26.5 m s^{-1} at 1537 LST. The remarkable temperature drop and strong gust occurred at 1537 LST signify-ing the passage of a strong gust front. A rainfall amount of 10.5 mm h^{-1} was reported at 1600 LST.
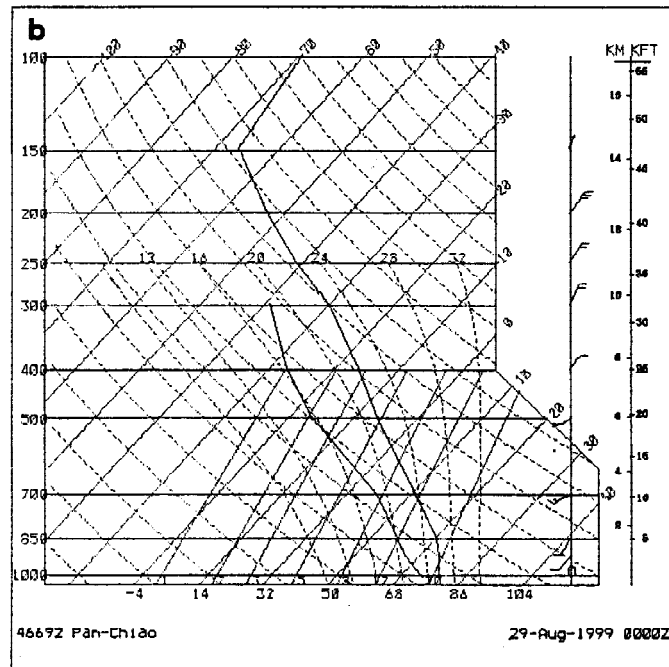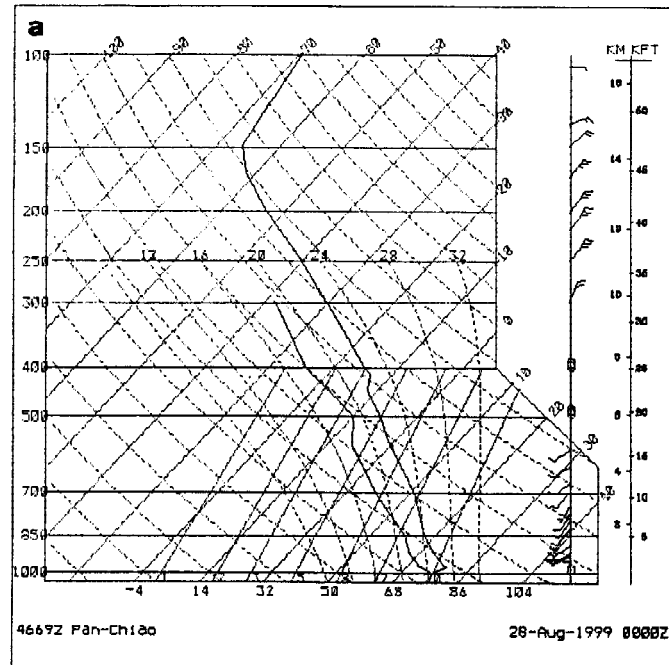
Fig. 4. Soundings at Pan-Chiao (Taipei) rawinsonde station at (a) 0000 UTC 28 August and (b) 0000 UTC 29 August 1999.
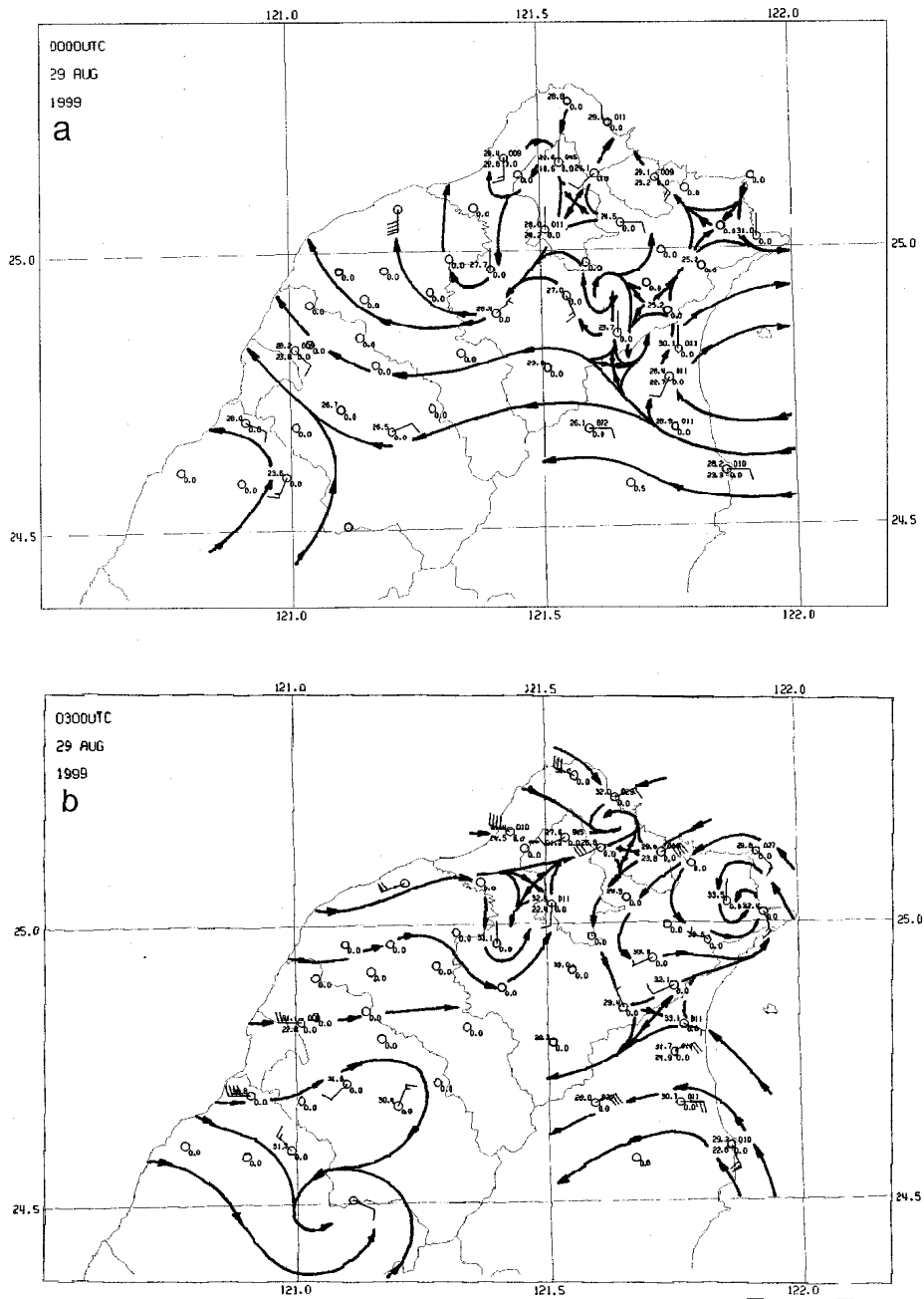
Fig. 5. Surface streamline and isohyet analyses at (a) 0000 UTC, (b) 0300 UTC, (c) 0600 UTC, (d) 0700 UTC, and (e) 0800 UTC 29 August 1999. A full wind barb indicates 1 m s^{-1}, half wind barb 0.5 m s^{-1}, and triangle flag 5 m s^{-1}. Dashed lines are isohyets in mm h^{-1}.
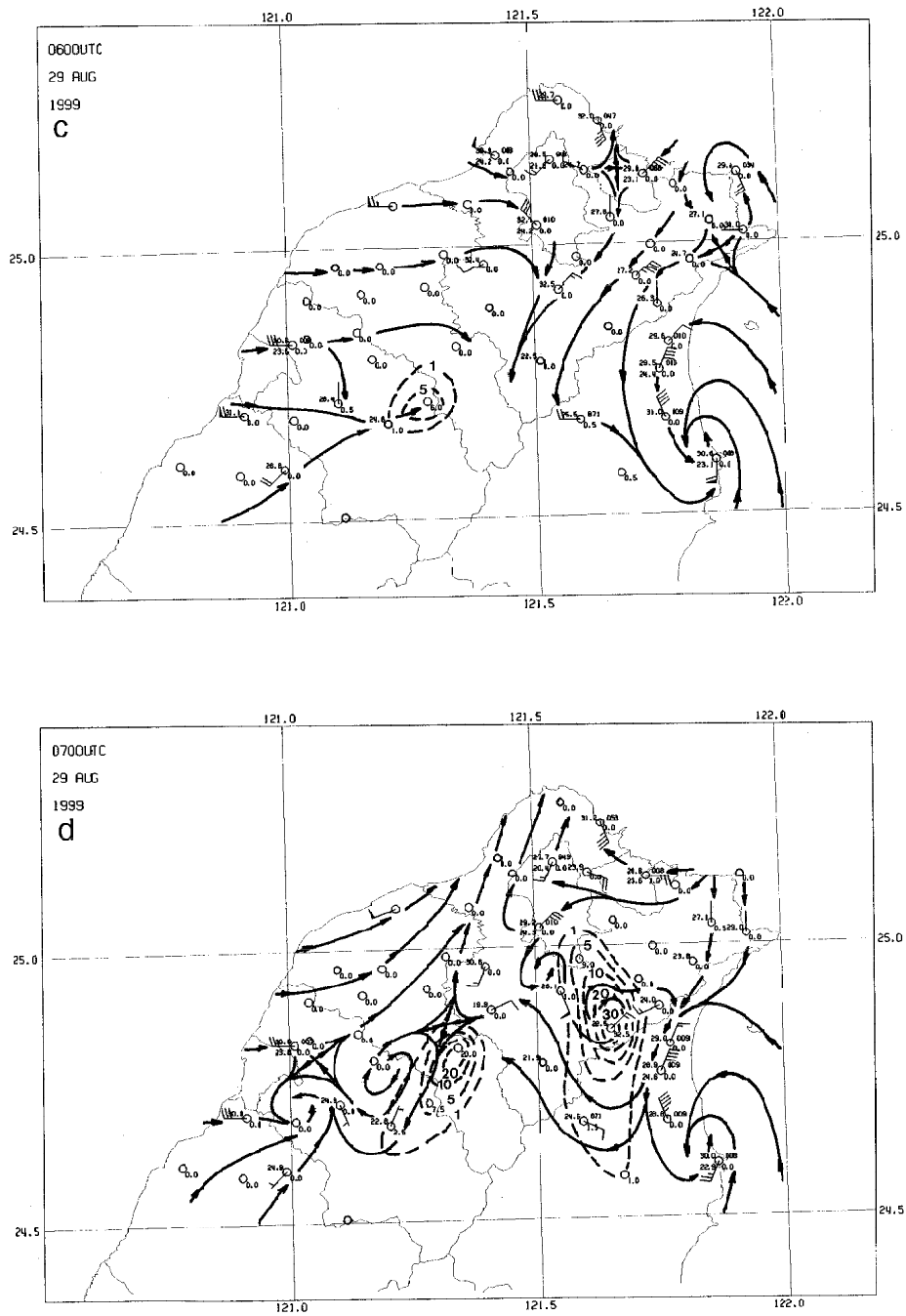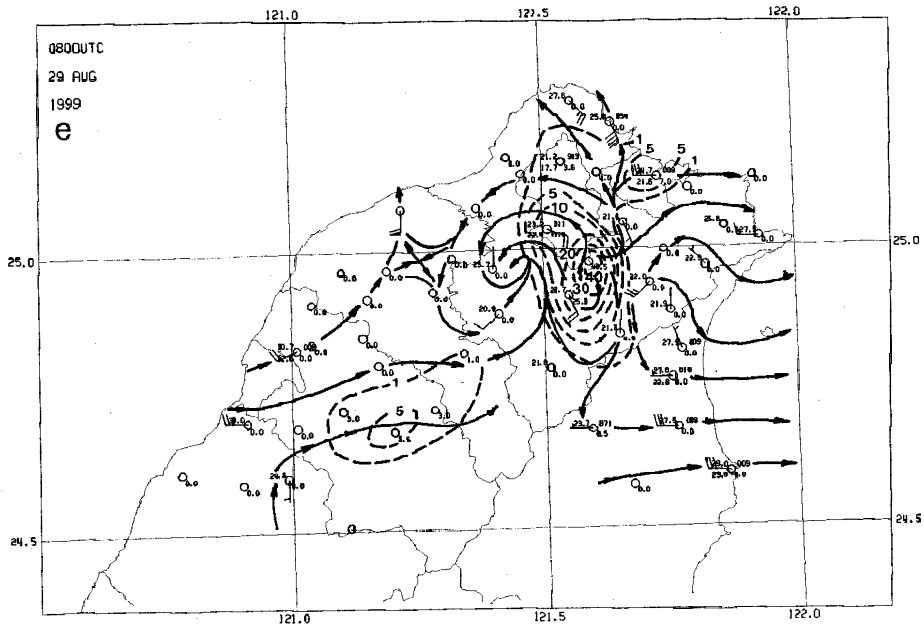
Fig. 5. Continued.
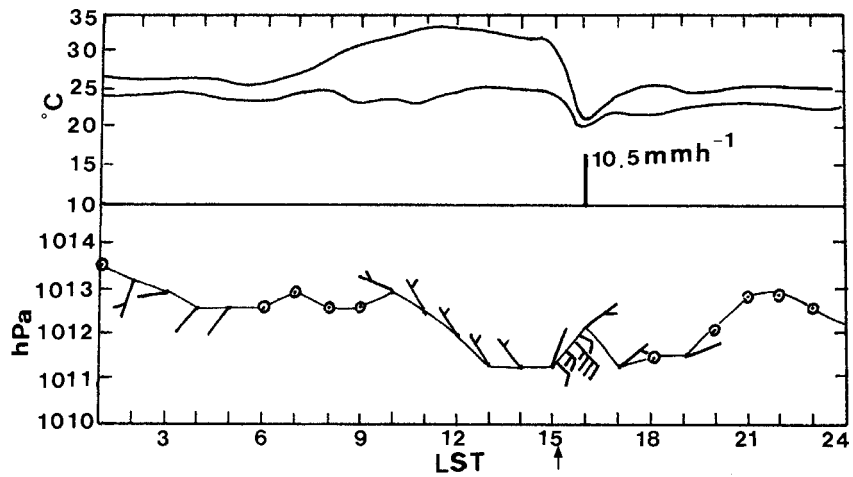
Fig. 5. Continued.

Fig. 6. Surface hourly observations of temperature, dew point, rainfall (upper panel), and pressure (lower panel) at Sung-Shan Airport in 0100 - 2400 LST 29 August 1999. A full wind barb indicates 5 m s^{-1} and half wind barb 2.5 m s^{-1}. Arrow indicates the passage time of gust front.

5. CHARACTERISTICS OF RADAR OBSERVATIONS

5.1 VMI Reflectivity

Figure 7 presents the spatial distribution of radar VMI reflectivity at 1300, 1500, and 1530 LST 29 August. At 1300 LST, convection mainly occurred over the SMR and its western slope. A NE-SW oriented line-type convective system was quite evident. It then developed and organized into a squall-line type mesoscale convective system (MCS) and moved north-westward to the northwestern slope of the SMR at 1500 LST. Convective cells developed along the leading edge over the western portion and the trailing stratiform region formed over
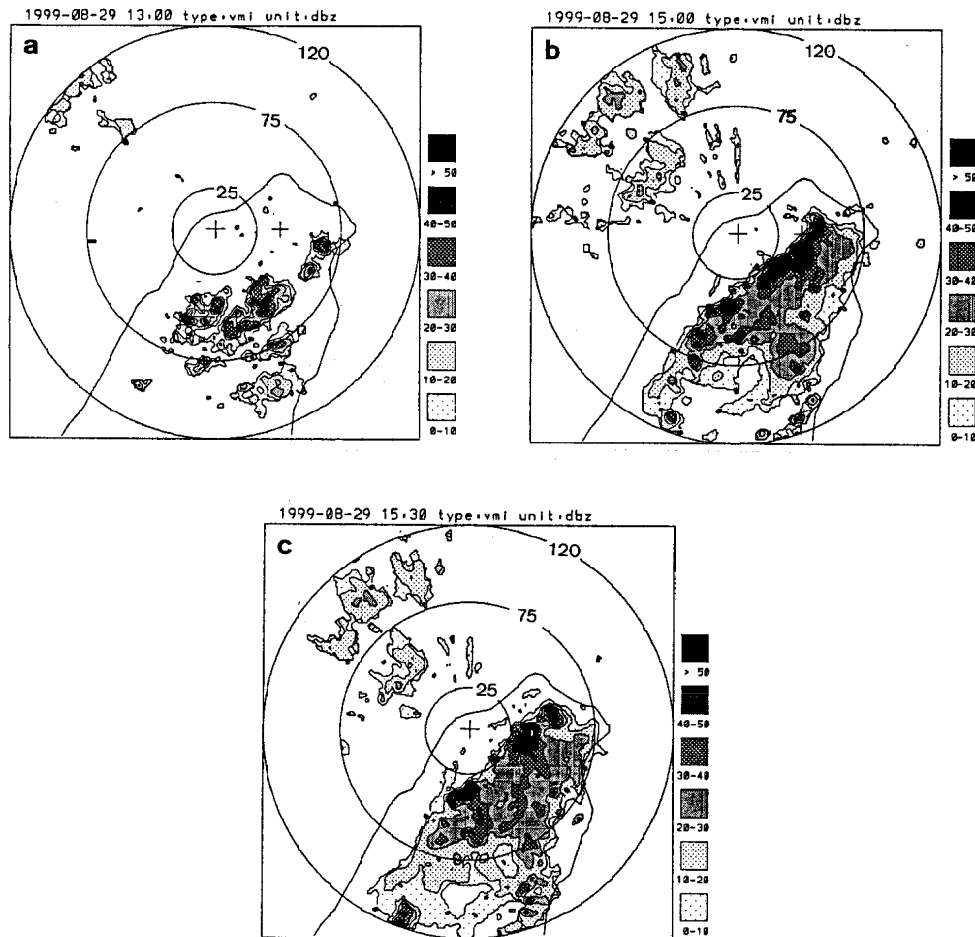

Fig. 7. Radar reflectivity (dBZ) of vertical maximum indicator (VMI) at (a) 1300 LST, (b) 1500 LST, and (c) 1530 LST 29 August 1999. The radius is 25, 75, and 120 km for inner, middle, and outer circle, respectively. Dashed lines indicate the vertical cross sections in Fig. 8.
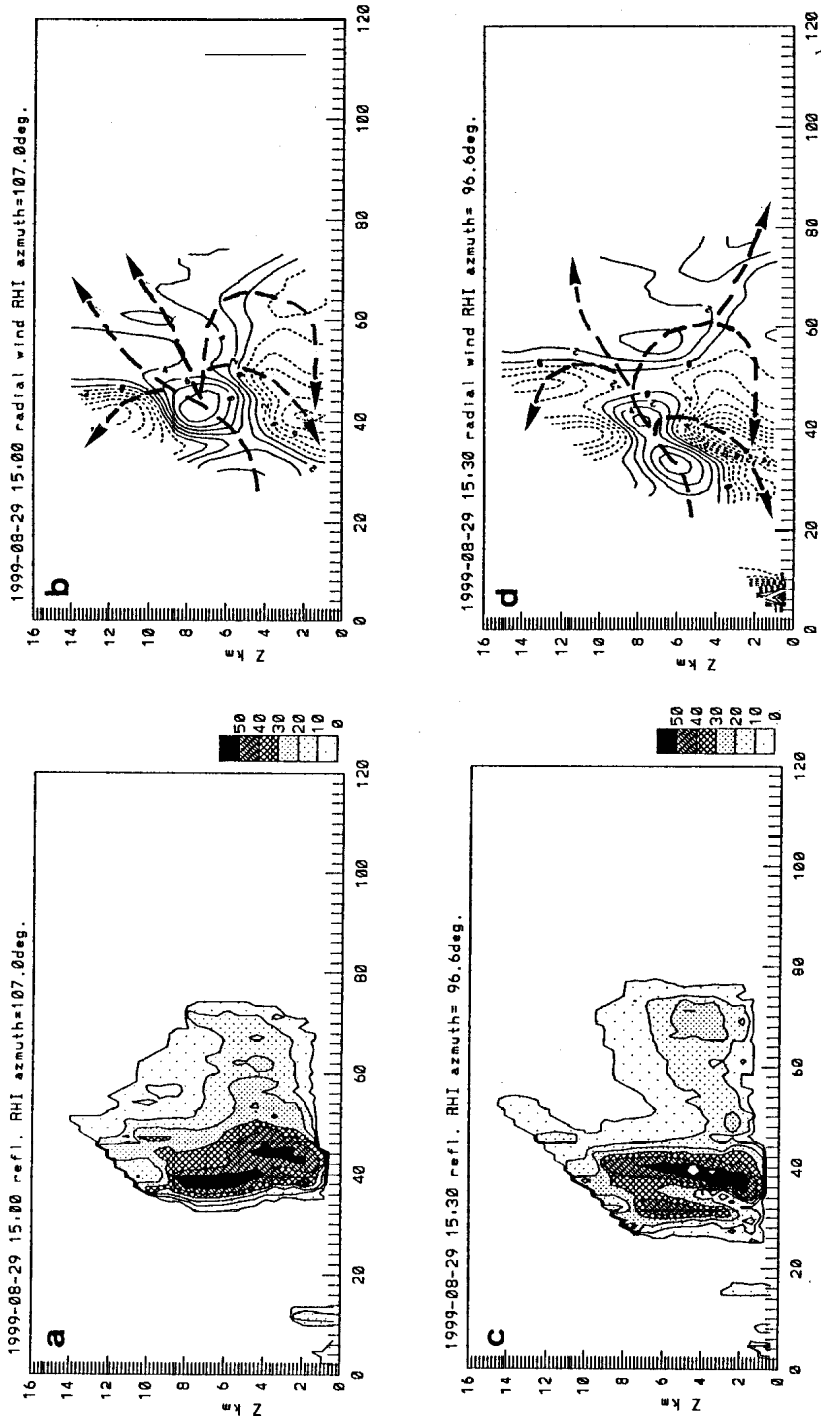
Fig. 8. RHI (range-height indicator) along 107° for (a) radar reflectivity (dBZ) and (b) radial wind at 1500 LST, and along 96.6° for (c) radar reflectivity and (d) radial wind at 1530 LST 29 August 1999. X axis indicates distance (km) from CKS International Airport (0 km) and Y axis indicates height (km). Contours of radial winds analyzed at $2 \, \mathbf{m \, s}^{-1}$ intervals with positive values (solid) away from radar and negative values (dashed) towards radar. Arrows illustrate the relative air flows as indicated by radial winds.

the eastern portion of this MCS. At 1530 LST, the convective cell located to the immediate south of the Sung-Shan Airport reached a maximum intensity of 63 dBZ. It produced heavy rainfall, hail, and strong gusts at the Sung-Shan Airport and its vicinities (Figs. 5e, 6).

5.2 RHI Observations

RHI reflectivity and radial wind across the convective system to the southeast of the CKS International Airport at 1500 and 1530 LST 29 August are presented in Fig. 8. At 1500 LST, the convective system was well developed with a maximum echo greater than 50 dBZ over the leading convective region which tilted vertically toward northwest. The front-to-rear inflow from low- and mid-troposphere was accompanied by upper-level outflows toward both the front and the rear of the system. The strong convective updraft core was located at about 40 km to the southeast of the radar site as indicated by strong upper-level divergent outflows. The very deep low-level outflows in this case were apparently produced by a convective downdraft under the leading convective region coupled with a mesoscale downdraft under the trailing stratiform region. The maximum cold air outflow was located below 2 km at about 40 km to the east of the radar site. Low-level outflows were also evident on the surface wind observations as presented in the mesoanalyses in Fig. 5d. It was essential in providing convergence and the resulting lifting for generating new convective cells in the leading edge and the northwestward propagation of the convective system. At 1530 LST, the system moved northwestward and intensified with a maximum intensity of 63 dBZ. The structure of radar reflectivity and radial wind was quite similar to that in the previous period except that the low-level outflow originating from the trailing stratiform precipitation toward the rear of system was evident at this time. Strong outflows from this convective system were again presented in the surface mesoanalyses in Fig. 5e and were observed at the Sung-Shan Airport with a strong gust of 26.5 m s^{-1} at 1537 LST (Fig. 6).

5.3 CAPPI Reflectivity

CAPPI reflectivity at 2 km from 1330-1530 LST 29 August is presented in Fig. 9. A NE-SW oriented line-type convection was located to the immediate south of the Sung-Shan Airport and intensified while moving northwestward during 1330 - 1430 LST. As the system continued to intensify, the squall-line type structure became more evident at 1500 LST with a convective leading edge and a trailing stratiform region (Fig. 9c). As indicated in the radial wind distribution on RHI along 107° (Fig. 8b), the convective updraft core was located at about 4 km to the south of the Sung-Shan Airport. The strong convective updraft occurred over the area of strong reflectivity gradient as would be expected. The convection reached a maximum intensity of 63 dBZ to the south of the Sung-Shan Airport at 1530 LST (Figs. 8c, 9d).

5.4 Radial Winds

Figure 10 presents PPI radial wind at 0.5° elevation angle at 1500 - 1600 LST 29 August. A mesocyclone formed as indicated by the dipole structure of positive and negative radial winds to

the south of the Sung-Shan Airport at 1500 LST. It then moved north-northwestward and intensified. The dipole structure of the vortex tended to rotate counterclockwise (Fig. 10b). The radial wind toward radar reached a maximum of 19.1 m s^{-1} at 1530 LST. Meanwhile, the mesocyclone also expanded as indicated by the increased distance between the dipole centers. At 1600 LST,
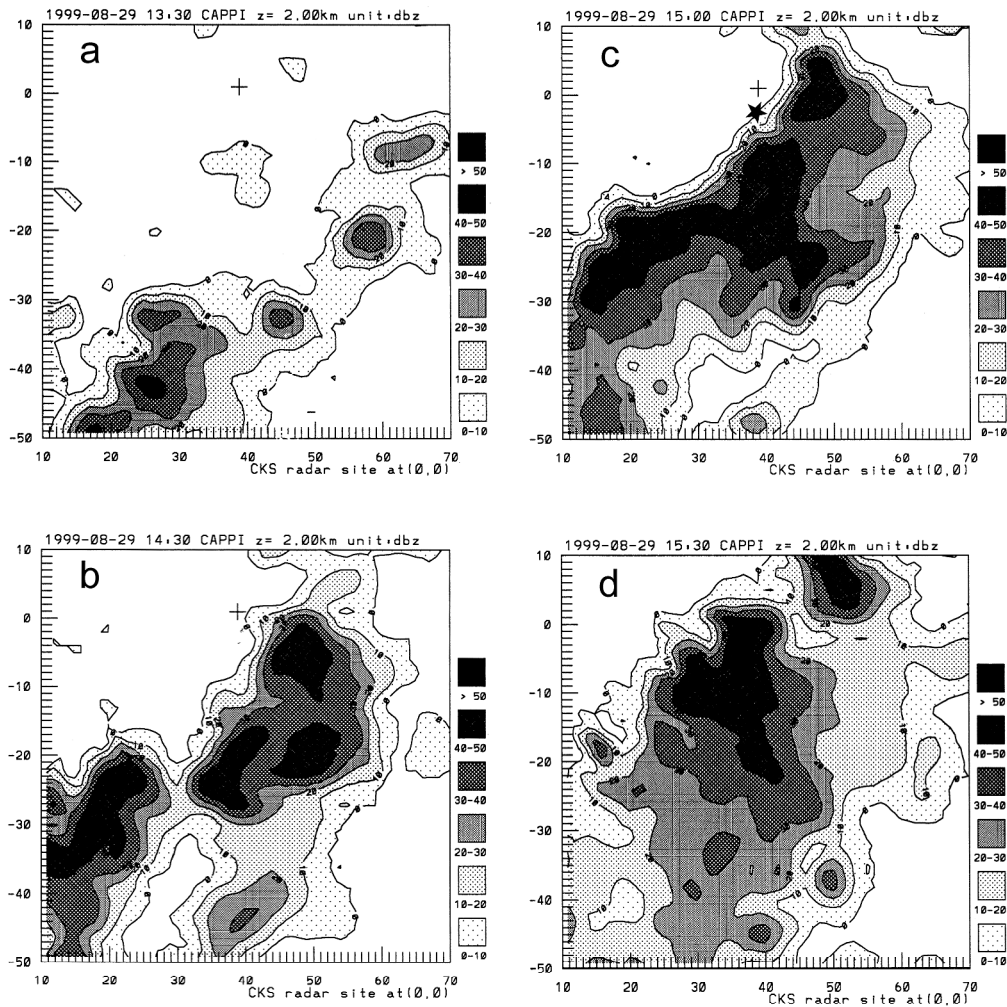

Fig. 9. CAPPI (constant altitude plan position indicator) radar reflectivity (dBZ) at 2 km for (a) 1330, (b) 1430, (c) 1500, and (d) 1530 LST 29 August 1999. X axis and Y axis are distances (km) in E-W and N-S direction. CKS International Airport is at (0,0) and symbol "+" indicates Sung-Shan Airport which was located at about 40 km to the east of CKS International Airport. Star sign in (c) indicates the location of the convective updraft core.

mesocyclone weakened although its dipole structure continued to rotate cyclonically and to expand while moving northwestward.

CAPPI radial winds for different altitudes at 1500 and 1530 LST 29 August are presented in Figs. 11 and 12, respectively. At 1500 LST, a mesocyclone was evident to the south of the Sung-Shan Airport at 0.5 and 2 km, to the northwest of the mesocyclone at 2 km, a mesoscale
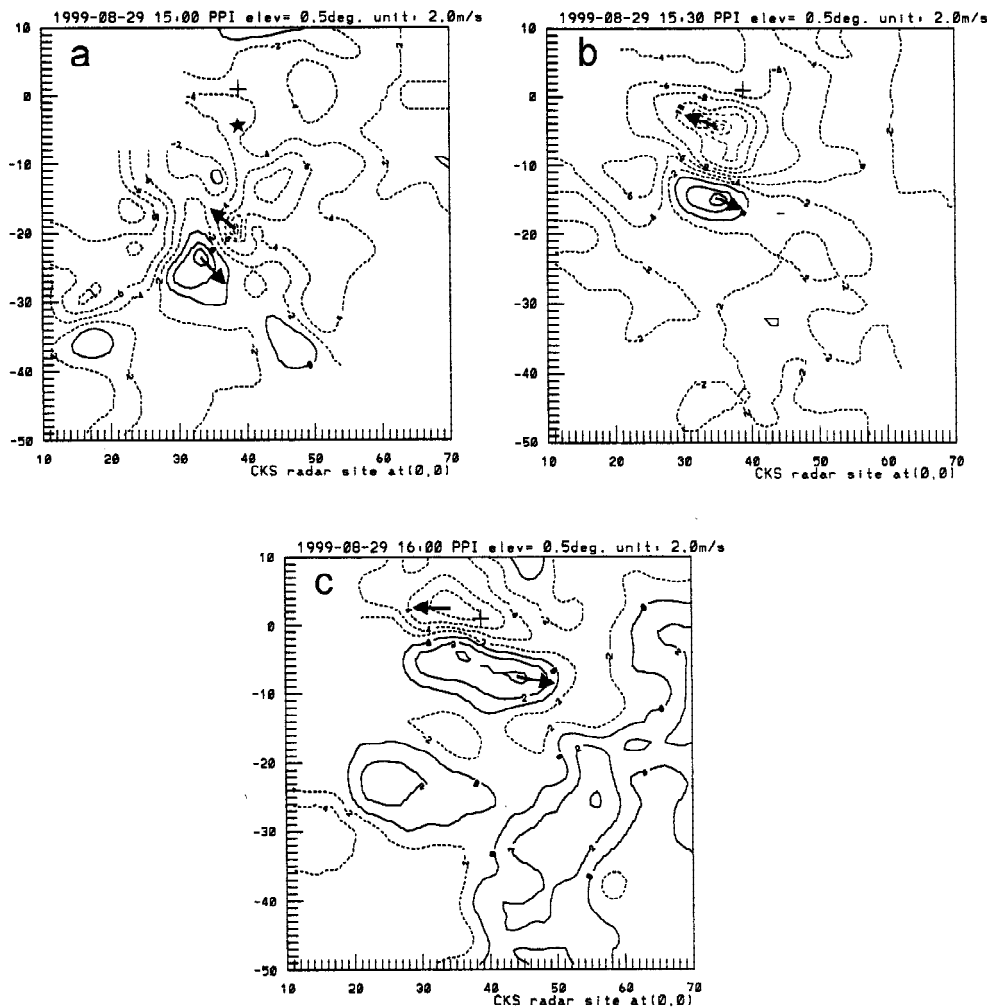

Fig. 10. PPI (plan position indicator) radial wind (m s^{-1}) at 0.5° elevation angle for (a) 1500, (b) 1530, and (c) 1600 LST 29 August 1999. Star sign indicates the location of the convective updraft core. Radial winds analyzed at 2 m s^{-1} intervals with negative values (dashed) towards radar and positive values (solid) away from radar. Arrows illustrate the radial wind directions at the centers of maximum radial wind.

anticyclone was evident. At 5 km, a mesoscale anticyclone occurred to the south of the Sung-Shan Airport. Convergence occurred to the southwest of the Sung-Shan Airport over the leading edge of the convective system (cf. Fig. 9c) at all altitudes analyzed in the low- and mid-troposphere (cf. Fig. 8b). At 1530 LST, the signatures of mesocyclone and mesoscale anticyclone were similar to those at 1500 LST. The northwestward movement of the low-level mesocyclone and its cyclonic rotation of the dipole structure were evident. Convergence again prevailed along the leading edge of the convective system to the southwest of the Sung-Shan Airport in the low- and mid-troposphere.
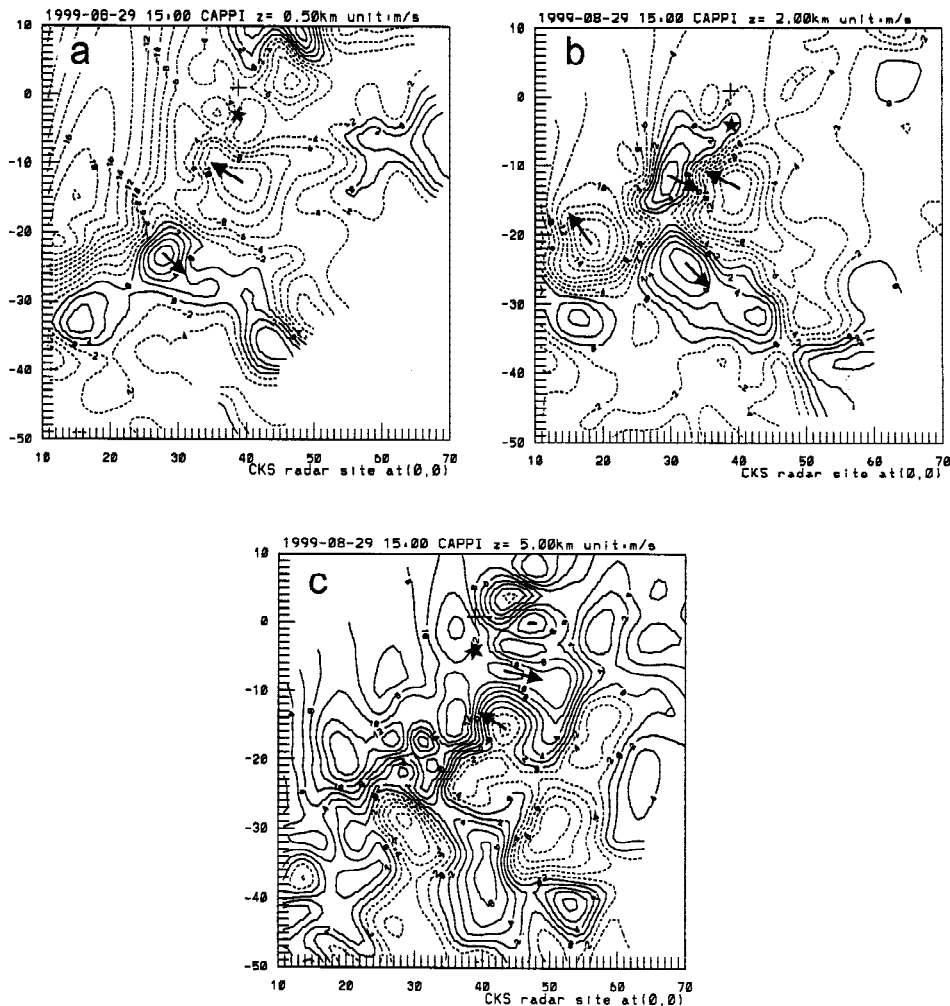

Fig. 11. As in Fig. 10, except for CAPPI radial wind (m s^{-1}) for (a) 0.5, (b) 2.0, and (c) 5.0 km at 1500 LST 29 August 1999.
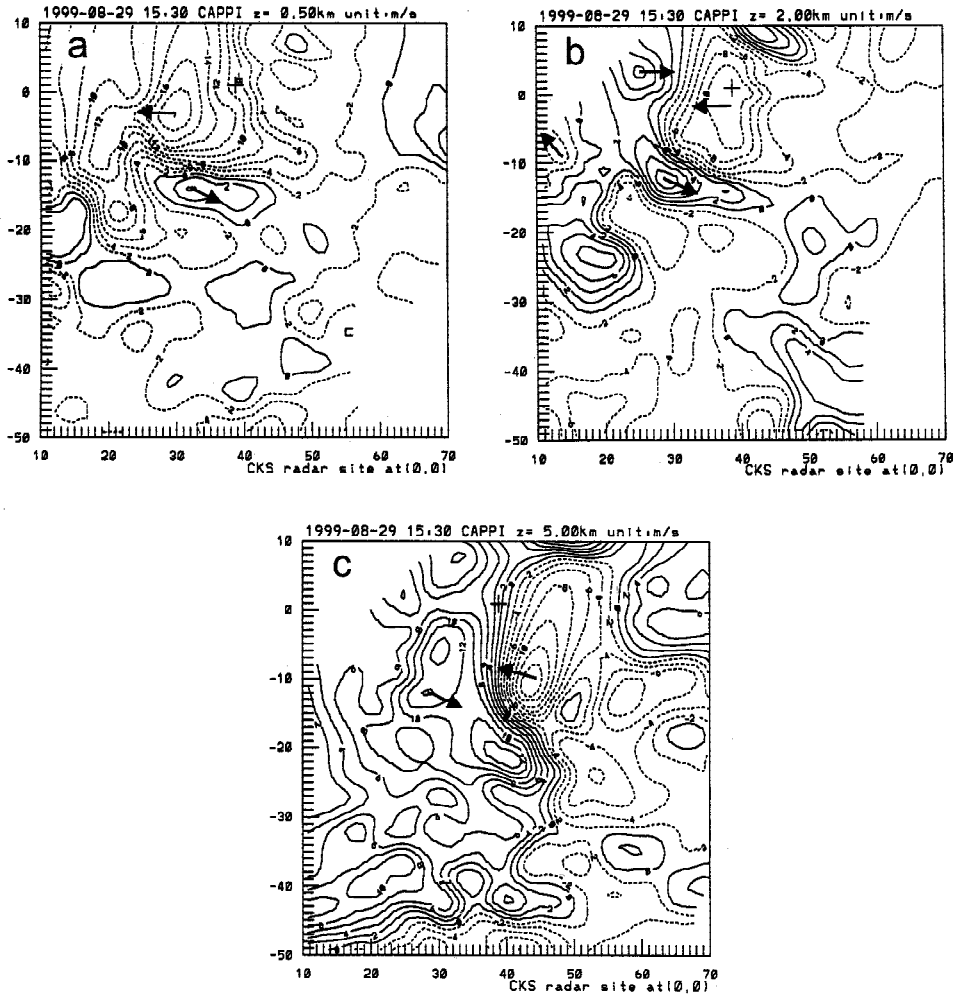
Fig. 12. As in Fig. 11, except at 1530 LST 29 August 1999.

6. DISCUSSION AND SUMMARY

A theoretical study by Klemp (1987) suggested that a cyclonic-anticyclonic couplet can be generated by tilting process on the vertical wind shear with a cyclonic vortex on the right-hand side and an anticyclonic vortex on the left-hand side of the vertical shear vector. It was also found that the pressure perturbation is related to the vertical shear with high pressure on the upstream and low pressure on the downstream of the vertical shear vector. The relationship among vortices, pressure perturbation, and vertical shear vectors as revealed by the Pan-Chiao rawinsonde station at 0000 UTC 29 August in this case is presented in Fig. 13. The anticyclonic (cyclonic) vortex formed to the northwest (southeast) of the strong updraft core and was

located on the left (right) hand side of the vertical shear vector (facing towards the direction) in the 1000 - 700 hPa layer. On the other hand, the anticyclonic (cyclonic) vortex formed to the southeast (northwest) of the strong updraft core and was located on the left (right) hand side of the vertical shear in the 700 - 400 hPa layer.

At 2 km, the mesoscale convergence over the area of strong updraft was estimated to be about 1.2×10^{-3} s^{-1} at 1500 LST. The strong updraft was then estimated to be 2.5 m s^{-1} and the vorticity generation through tilting process was estimated to be 1.5×10^{-6} s^{-2} in this case. Thus, it only needed 25 minutes to generate a low-level vortex of 2.4×10^{-3} s^{-1} as observed in Fig. 11b. If the mesocyclone at 2 km was generated through the vortex stretching process by the mesoscale convergence, it would need about 9 hours to generate the vortex intensity observed at 1500 LST in this case. Therefore, the mesovortices in the low level were suggested to be generated by the convective updraft on the vertical wind shear through tilting process. At 1500 LST, the existence of a couplet of cyclonic-anticyclonic vortices at 2 km was consistent with
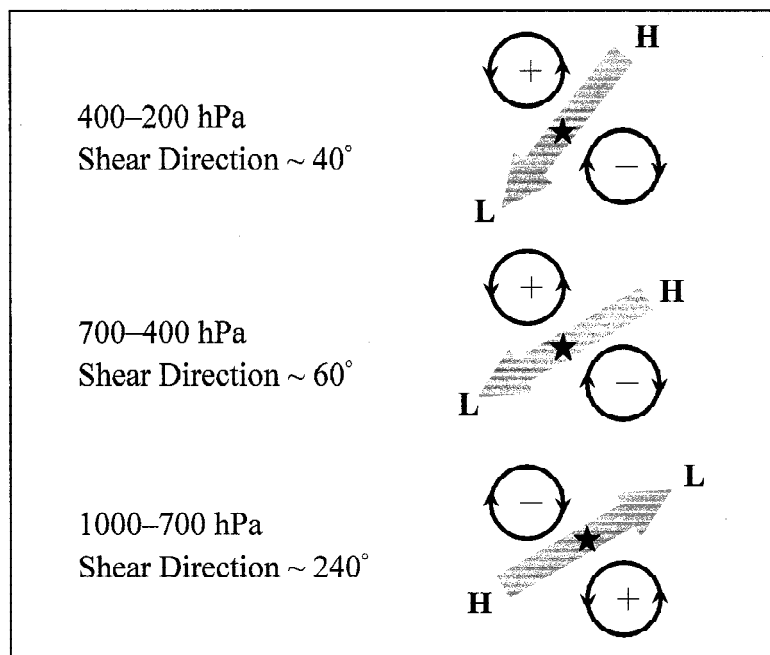

Fig. 13. Pressure perturbation and vorticity perturbation generated by vertical wind shear and convective updraft core in each layer at 0000 UTC 29 August 1999. Arrows indicate vertical shear directions. "H" and "L" indicate the high and low perturbation pressure, respectively. Circles illustrate vorticity perturbation with plus sign for cyclonic and minus sign for anticyclonic circulation. Star sign indicates the location of the convective updraft core.

the vertical shear in the lower troposphere as would be expected theoretically from the morning sounding at Pan-Chiao rawinsonde station observed at 0000 UTC (0800 LST) on the same day (Fig. 13). At 5 km, the estimated mesoscale convergence of 2.0×10^{-3} s^{-1} would suggest the strong updraft of 8.5 m s^{-1}. It only took about 5 minutes to generate the anticyclonic vortex (Fig. 11c) through tilting process. The vortices in this case were different from those vortices frequently observed in mesoscale convective systems at a horizontal scale of 100 - 200 km, which can be explained by balanced dynamics (Davis and Weisman 1994).

The westward propagation and intensification of the convective system were also supported by an upward perturbation pressure gradient over the area to the southwest of the strong updraft core. On the other hand, convection over the area to the northeast was suppressed by the downward perturbation pressure gradient. Therefore, the increase of vertical shear under the influence of the upper-level cold vortex appeared to be a supportive factor for the westward propagation and intensification of the convective storm in this case.

Environmental conditions and local circulations involved in the development of a severe convective system, which produced hail and strong gusts in the Taipei Basin, were analyzed for the case of 29 August 1999. Doppler radar observations at the CKS International Airport were used to reveal the structure and behavior of the convective system and the resultant mesoscale vortices. Results are summarized as follows:

1) The upper-level cold vortex to the southeast of Taiwan provided favorable conditions for the development of strong convection. These included an increase in north-northeast wind and vertical wind shear, and an increase in potential instability by lowering temperature in the upper troposphere.

2) Drying of the mid-troposphere was primarily responsible for the strong outflows and strong gust as the mid-level front-to-rear inflows entered the system and caused strong evaporative cooling.

3) Sea breezes/upslope winds and the convergence line were important factors for triggering convection under a rather weak synoptic-scale flow.

4) The outflows produced by the convective system over the western slope of the Snow Mountain Range interacted with sea breezes/upslope winds. This was responsible for the formation of the new convection in the leading edge of the system and the northwestward propagation of the system.

5) The upward dynamic pressure gradient associated with the increase of vertical shear under the influence of an upper-level cold vortex appeared to be a supportive factor for the westward propagation and intensification of this convective system.

6) The mesoscale vortices formed in the low- and mid-troposphere in the convective system which produced hail and gust. They appeared to be generated by the tilting process under the conditions of increased vertical wind shear and the existence of a strong convective updraft.

REFERENCES

Chen, G. T. J., L. F. Chen, and L. F. Chou, 1990: A study on the upper-tropospheric cold vortices: Cases accompanying thunderstorms. *Proc. Conf. on Weather Radar and Flight Safety*, Civil Aeronautics Administration, Taipei, Taiwan, 329-349. (in Chinese with English Abs.)

Davis, C. A., and M. L. Weisman, 1994: Balanced dynamics of mesoscale vortices produced in simulated convective systems. *J. Atmos. Sci.*, **51**, 2005-2030.

Klemp, J. B., 1987: Dynamics of tornadic thunderstorms. *Ann. Rev. Fluid Mech.*, **19**, 369-402.

Newton, C. W., and H. R. Newton, 1959: Dynamical interactions between large convective clouds and environment with vertical shear. *J. Meteor.*, **16**, 483-496.

Rotunno, R., J. B. Klemp, and M. L. Weisman, 1988: A theory for strong, long lived squall lines. *J. Atmos. Sci.*, **45**, 463-485.

Weisman, M. L., 1992: The role of convectively generated rear-inflow jets in the evolution of long-lived mesoconvective systems. *J. Atmos. Sci.*, **49**, 1826-1847.

Weisman, M. L., and J. B. Klemp, 1982: The dependence of numerically simulated convective storms on vertical wind shear and buoyancy. *Mon. Wea. Rev.*, **110**, 504-520.

Zipser, E. J., 1977: Mesoscale and convective-scale downdrafts as distinct components of squall-line circulation. *Mon. Wea. Rev.*, **105**, 1568-1589.